# Multi-Elliptic Rogue Wave Clusters of the Nonlinear Schrodinger Equation on Different Backgrounds

**Stanko N Nikolic** ( stankon@ipb.ac.rs )
Texas A&M University at Qatar https://orcid.org/0000-0002-2082-9954
**Sarah Al Washahi**
Faculty of Physics, University of Belgrade
**Omar A. Ashour**
University of California Berkeley
**Siu A. Chin**
Texas A&M University College Station: Texas A&M University
**Najdan B. Aleksic**
TAMUQ: Texas A&M University at Qatar
**Milivoj R. Belic**
TAMUQ: Texas A&M University at Qatar

**Research Article**

**Keywords:** Nonlinear Schrödinger equation, Rogue waves, Circular and triangluar rogue wave clusters, Darboux transformation

**Posted Date:** December 1st, 2021

**DOI:** https://doi.org/10.21203/rs.3.rs-1116823/v1



**Version of Record:** A version of this preprint was published at Nonlinear Dynamics on January 11th, 2022. See the published version at https://doi.org/10.1007/s11071-021-07194-5.

**Noname manuscript No.**
(will be inserted by the editor)

# Multi-elliptic rogue wave clusters of the nonlinear Schrödinger equation on different backgrounds

**Stanko N. Nikolić · Sarah Al Washahi · Omar A. Ashour · Siu A. Chin · Najdan B. Aleksić · Milivoj R. Belić**

Received: date / Accepted: date

**Abstract** In this work we analyze the multi-elliptic rogue wave clusters as new solutions of the nonlinear Schrödinger equation (NLSE). Such structures are obtained on uniform backgrounds by using the Darboux transformation scheme of order $n$ with the first $m$ evolution shifts that are equal, nonzero, and eigenvalue-dependent, while the imaginary parts of all eigenvalues tend to one. We show that an Akhmediev breather of $n-2m$ order appears at the origin of the $(x,t)$ plane and can be considered as the central rogue wave of the cluster. We show that the high-intensity narrow peak, with characteristic intensity distribution in its vicinity, is enclosed by $m$ ellipses consisting of the first-order Akhmediev breathers. The number of maxima on each ellipse is determined by its index and the solution order. Since rogue waves in nature usually appear on a periodic background, we utilize the modified Darboux transformation scheme to build these solutions on a Jacobi elliptic dnoidal background. We analyze the minor semi-axis of all ellipses in a cluster as a function of an absolute evolution shift. We show that the cluster radial symmetry in the $(x,t)$ plane is violated when the shift values are increased above a threshold. We apply the same analysis on Hirota equation, to examine the influence of a free real parameter and Hirota operator on the cluster appearance. The same analysis can be extended to the infinite hierarchy of extended NLSEs.

**Keywords** Nonlinear Schrödinger equation · Rogue waves · Circular and triangluar rogue wave clusters · Darboux transformation

S. N. Nikolić
Science Program, Texas A&M University at Qatar, P.O. Box 23874 Doha, Qatar
Institute of Physics Belgrade, University of Belgrade, Pregrevica 118, 11080 Belgrade, Serbia
E-mail: stankon@ipb.ac.rs

S. Al Washahi
Faculty of Physics, University of Belgrade, Studentski trg 12, 11001 Belgrade, Serbia
Faculty of Science Al-Zawiya, University of Libya, Al Ajaylat, Libya

O. A. Ashour
Department of Physics, University of California, Berkeley CA 94720, USA

S. A. Chin
Department of Physics and Astronomy, Texas A&M University, College Station, TX 77843, USA

N. B. Aleksić
Moscow State Technological University "STANKIN", Moscow, Russia
Science Program, Texas A&M University at Qatar, P.O. Box 23874 Doha, Qatar

M. R. Belić
Science Program, Texas A&M University at Qatar, P.O. Box 23874 Doha, Qatar

## 1 Introduction

The cubic nonlinear Schrödinger equation (NLSE) [1–3] has been widely studied due to its huge importance in analyzing physical systems in various fields, such as nonlinear optics [4–8], Bose−Einstein condensates [9, 10], oceanography [11,12], plasmas [13], etc. The simple cubic one-dimensional NLSE that will be mostly considered in this work has the form:

$$i\psi_x + \frac{1}{2}\psi_{tt} + |\psi|^2\psi = 0. \tag{1.1}$$

The transverse spatial variable is denoted by $t$, the retarded time in the moving frame by $x$, while the

slowly-varying envelope corresponds to the wave function $\psi \equiv \psi(x,t)$. This form of NLSE is appropriate for the propagation of light pulses in fibers.

In recent times, the extended family of nonlinear Schrödinger equation (ENLSE) that may include infinite number of higher-order dispersion terms with additional nonlinearities has been proposed and investigated in [14,15]. The extension of NLSE to the hierarchy of higher-order equations originated from the need to explain the propagation of ultrashort pulses through optical fibers [16,17]. So far, the attention was mostly focused on Hirota [18,19] (with third-order dispersion) and quintic equation (comprising the dispersions up to the fifth-order) [20–23].

Both the NLSE and its extended variants exhibit similar classes of solutions, among which the most important seem to be Akhmediev breathers (AB) [24,25] and different solitons [26]. An AB consists of a series of intensity maxima on a finite background that are localized in time and periodic in space. The term soliton in general describes a solitary wave packet that propagates along some direction in the $(x,t)$ plane on a zero background without distortion in its shape. The technique that is often used to derive exact analytical solutions is the Darboux transformation (DT) [27]. It utilizes the Lax pair formalism and recursive relations to calculate higher-order solutions of the NLSE starting from the trivial zeroth-order seed function which satisfies Eq. (1.1).

The importance of DT for this work is its ability to provide higher-order Akhmediev breathers on uniform [28] and periodic backgrounds [29,30]. The breather emerges as a high intensity narrow peak with a complex intensity distribution at its base. Such structures can be considered as rogue waves (RWs), which "appear from nowhere and disappear without a trace". The RW is localized both in space and time and is defined by one dominant peak. The simplest example of a RW is the Peregrine soliton [31]. The notion of rogue waves is now widely spread around, in studies of deep ocean waves [12,32], nonlinear optics [33,34], superfluidity [35], Bose-Einstein condensates [36], and others. The current hot topic in the nonlinear science is to investigate the cause and nature of rogue waves [37]. This research is attracting more attention as well because a new scheme for RWs excitation, via the electromagnetically induced transparency (EIT) [38–40], was described recently [41].

In this work we investigate the special multi-elliptic rogue wave clusters of the NLSE. These solutions are also periodic along $t$-axis and throughout the paper we consider the intensity distribution within a single transverse period. It consists of a rogue wave peak (ABs of the second-order or higher), surrounded by the first-order ABs positioned on a number of concentric ellipses centered on the peak (see Fig. 1). We obtain these structures on uniform and Jacobi elliptic dnoidal backgrounds, by using the DT of order $n$, having the first $m$ evolution shifts equal, nonzero, and eigenvalue-dependent. We show that the order of the central rogue wave and the number of ellipses are determined by the two mode numbers, $n$ and $m$.

Various multi-rogue wave solutions have been previously analyzed as triplets [42], triangular cascades [43–45], and circular clusters [28,46,47]. The classification of various hierarchy of multi-RW structures into families was presented in [48,49]. Our results are similar to those in [50]. Here however, we adopt a different scheme for generating such clusters by using evolution shifts in the Darboux scheme. We further analyze the semi-axes of ellipses as functions of these shifts and estimate when the radial symmetry will break up. We further show how to generate elliptic RW clusters on a dn background, which was not considered before. In addition, we generalize our results, by producing such solutions for the Hirota equation as well, and point to ways how to generalize this analysis to the infinite hierarchy of NLSEs.

This paper is organized as follows. In Sec. 2, we briefly discuss the main properties of higher-order Akhmediev breathers. In Sec. 3, we present various NLSE solutions in the form of multi-elliptic rogue wave clusters on a uniform background. In Sec. 4, we analyze the lengths of semi-axes of elliptical rings, by going up to four ellipses in the cluster. In Sec. 5, we exhibit the NLSE cluster solutions on a Jacobi elliptic dnoidal background. In Sec. 6, we generalize our findings to Hirota equation that includes the third-order dispersion and additional nonlinearities. In Sec. 7, we summarize our results.

## 2 Higher-order Akhmediev breathers

Here we briefly describe Akhmediev breathers of the NLSE and how to use DT scheme to generate higher-order RW solutions. The first-order AB is a single-periodic function along the $t$-axis [24,25]:

$$\psi(t,x) = \left[1+\frac{2(1-2a)\cosh\lambda x + i\lambda\sinh\lambda x}{\sqrt{2a}\cos\omega t - \cosh\lambda x}\right]e^{ix}. \qquad (2.1)$$

The period $L$ and the angular frequency $\omega$ of AB of any order are determined by a single parameter $a$, with $0 < a < 0.5$ [51]:

$$L = \frac{\pi}{\sqrt{1-2a}}, \qquad (2.2)$$

$$\omega = 2\sqrt{1-2a}. \tag{2.3}$$

AB turns into the Peregrine RW for $a = 0.5$ and becomes the Kuznetsov-Ma soliton when $a > 0.5$. An arbitrary AB can be derived using the DT, starting from the seed solution $\psi_0 = e^{ix}$. The $n$-th order AB (its wave function $\psi_n(x,t)$) turns out to be a nonlinear superposition of $n$ first-order ABs, each characterized by the complex eigenvalue $\lambda_j = r_j + i\nu_j$ and the evolution $x_j$, and spatial shifts $t_j$ ($j = 1, ..., n$). The existence of such abundance of relevant parameters offers an incredible variety of possible RW solutions. The Lax pair procedure and recursive relations in DT scheme that are used to calculate $\psi_n(x,t)$ from $\psi_0$ are described in details in [28]. It is important to note that the imaginary part $\nu$ of AB is simply related to the parameter $a$: $\nu = \sqrt{2a}$. By taking into account relation (2.3) one can see that the imaginary part of AB's eigenvalue is completely determined by its angular frequency: $\nu = \sqrt{1-\omega^2/4}$.

## 3 Multi-elliptic rogue wave clusters on uniform background

To generate multi-elliptic RW clusters, we require that the frequencies of constituent single-order breathers are all different, but close to zero. This goal can be achieved by defining them as harmonics of $\omega_1 = \omega \to 0$ so that $\omega_j = j\omega$, where $j \geq 2$ [28]. In this work, we take the simplest possibility that all real parts $r_j = 0$. The $n$ ABs are thus formed using their imaginary parts calculated from the corresponding frequencies:

$$\nu_j = \sqrt{1 - \frac{j^2\omega^2}{4}} \quad (1 \leq j \leq n). \tag{3.1}$$

It is easy to see that all $\nu_j$ tend to 1. Having set the eigenfrequencies, it remains to choose the evolution and spatial shifts. Different choices lead to very different solutions. We introduce a slight modification with respect to [28]: The first $m$ evolution shifts $x_j$ are set to be equal, nonzero, and eigenvalue-dependent. We assume them to be given via an expansion

$$x_j = \sum_{l=1}^{\infty} X_{jl}\omega^{2(l-1)} = X_{j1} + X_{j2}\omega^2 + X_{j3}\omega^3 + X_{j4}\omega^6 + \cdots \tag{3.2}$$

for $j \leq m$, and $x_j = 0$ for $j > m$. In addition, we simply set all $t_j$ shifts to be zero. We also assume that all $X_{jl} = 0$ except one particular value that is explicitly stated in the text. Although seemingly an oversimplification, this choice of parameters nonetheless leads to an interesting family of new RW clusters. And, as mentioned, all this is provided for by an incredible richness in the choice of four sets of parameters.

It turns out that such an $n$-th order Darboux solution with $m$ nonzero shifts $x_j$ is characterized by a single Akhmediev breather of order $n-2m$ placed at the origin $(0,0)$ (a central rogue wave, labeled as $\mathrm{RW}_{n-2m}$) and $m$ ellipses (rings) around the RW. The outer ellipse contains $2n-1$ ABs of order 1 (AB1), and each following ring towards the center has four AB1s less, as analyzed in [48,50]. We term this Darboux solution as the multi-RW cluster.

In Fig. 1 we present the multi-rogue wave cluster on uniform background having 2 ellipses. Hence, we set $m = 2$ and vary the value of $n$ in order to change the order of the central RW. The main frequency $\omega$ is set to $10^{-1}$. In Fig. 1a we set $n = 6$ and obtain the second-order RW at the center. The outer and inner ellipses consist of $c_1 = 11$ and $c_2 = 7$ AB1, respectively. In Fig. 1b, we set $n = 7$ to get a third-order RW. The number of AB1 on two ellipses is $c_1 = 13$ and $c_2 = 9$. One can further increase $n$ to get higher-order RWs that are rarely or never seen before. For $n = 8$, the RW4 is obtained with $c_1 = 15$ and $c_2 = 11$ (Fig. 1c). For $n = 9$, the RW5 is formed with $c_1 = 17$ and $c_2 = 13$ (Fig. 1d). It is seen that higher the order of the central RW, narrower and stronger the RW peak at $(0,0)$. The highest intensities in Figs. 1a-d are, respectively: 22.98, 44.45, 77.26, and 105.81. We have also computed solutions with other frequencies, for instance $\omega = 0.05$. The appearance of this RW cluster was very similar to the $10^{-1}$ case (not shown), so we proceeded with the 0.1 value.

In Fig. 2 we show the elliptic rogue wave cluster with 3 ellipses. Thus, we take $m = 3$ and change the $n$ value. In Fig. 2a we set $n = 8$ and obtain the second-order RW at $(0,0)$. The outer, middle, and inner ellipse consists of $c_1 = 15$, $c_2 = 11$, and $c_3 = 7$ AB1s, respectively. In Fig. 2b, $n = 9$ and a RW3 was observed with $c_1 = 17$, $c_2 = 13$, and $c_3 = 9$. The RW4 with $c_1 = 19$, $c_2 = 15$, and $c_3 = 11$ is computed for $n = 10$ (Fig. 2c).

We last show the results for $m = 4$. The analysis is analogous to the previous two cases. When $n = 10$, we get RW2 and 4 rings surrounding the central peak. The number of AB1 on four ellipses, from outer to the inner, is $c_1 = 19$, $c_2 = 15$, $c_3 = 11$, and $c_4 = 7$, respectively (Fig. 3a). Next, we take $n = 11$ and obtain RW3 with $c_1 = 21$, $c_2 = 17$, $c_3 = 13$, and $c_4 = 9$ (Fig. 3b).

In general, under conditions for DT computation presented in this section, our conjecture is that the RW of $n-2m$ order is obtained at $(0,0)$ with $m$ ellipses around the peak for $n \geq 2m+2$. If we index the rings from 1 to $m$, going from the outer to the inner one, then the number of AB1 on each ring is $c_i = 2n - 4i + 3$.

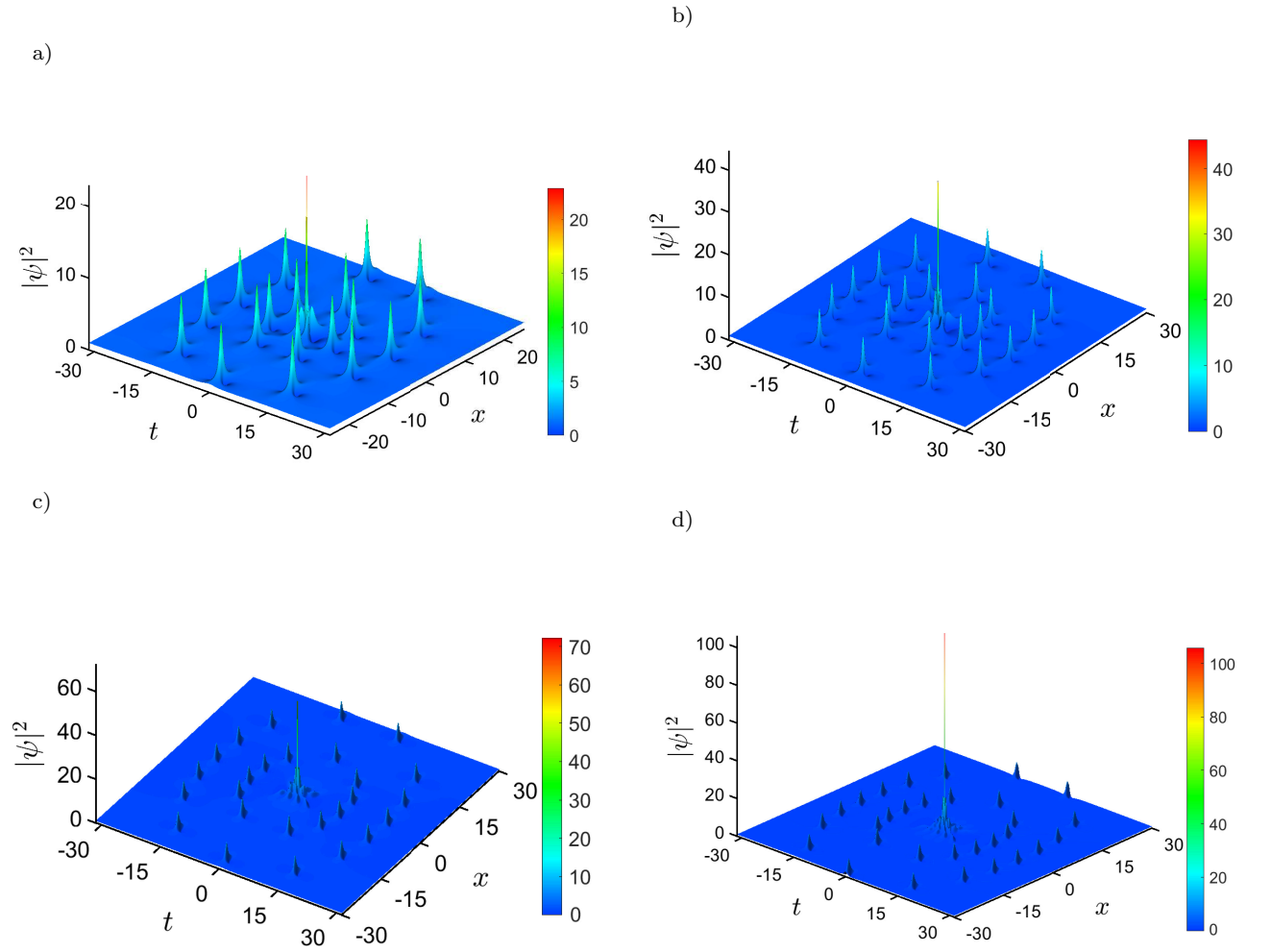


Fig. 1: Double-elliptic rogue wave clusters ($m = 2$) on the uniform background. The rogue wave of order $n - 2m$ is formed at the origin $(0, 0)$ of the $(x, t)$ plane. The shifts are calculated for $X_{j4} = 10^6$. The orders of Darboux transformation and the Akhmediev breather representing the high intensity central peak are: (a) $n = 6$ with the second-order rogue wave, (b) $n = 7$ with the third-order rogue wave, (c) $n = 8$ with the fourth-order rogue wave, and (d) $n = 9$ with the fifth-order rogue wave.

## 4 The semi-axes of ellipses in clusters

In paper [28], dealing with a single circular rogue wave cluster, authors proposed a formula for the radius of the ring depending on Darboux shifts along $x$ and $t$-axes. Having ellipses at hand, we present how the length of the vertical semi-axis depends on an absolute evolution shift for all ellipses, up to four rings ($m = 4$) in the cluster. In Fig. 4 we show the $n = 10$ and $m = 4$ case and indicate the AB1s on an $i$-th ellipse with numbers $i = 1$ to $i = 4$ (from the inner-most towards the outer-most ring). It turns out that all rings, for any $m$, have AB1s at $t = 0$ with alternating positions along this vertical line: the inner-most AB1 is positioned above the central RW. The next AB1 with index 2 is below the maximum at (0,0), the AB1 marked 3 is in the upper half of the $(x, t)$ plane, and so on. We therefore define the length of the vertical semi-axis $R_{xi}$ as the distance between the central RW at the origin and AB1 indexed with $i$. Since the higher-order DT solution is expressed by a very complicated and cumbersome analytical expression, which is difficult to write and analyze, we applied the numerical calculation of AB1 positions along the $t = 0$ line.

In Fig. 5a we show the $R_x$ dependence on $x_{\text{shift}} = x_1 = ... = x_m$ for two rings surrounding RW2 at the center ($n = 6,\ m = 2$) at two main frequencies: $\omega = 0.1$ and $\omega = 0.05$. We see that the position of AB1 at the first ring is increasing as the evolution shift becomes larger, in contrast to AB1's $x$-coordinate on the outer

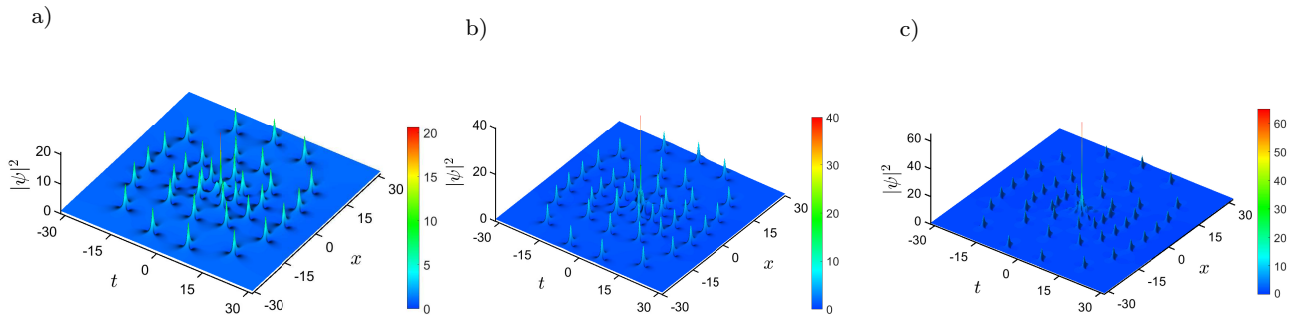


Fig. 2: Triple-elliptic rogue wave clusters ($m = 3$) on the uniform background ($X_{j4} = 10^6$). The rogue wave of order $n - 2m$ is formed at the origin $(0, 0)$ of the $(x, t)$ plane. The orders of Darboux transformation and the Akhmediev breather representing the high intensity central peak are: (a) $n = 8$ with the second-order rogue wave, (b) $n = 9$ with the third-order rogue wave, and (c) $n = 10$ with the fourth-order rogue wave.

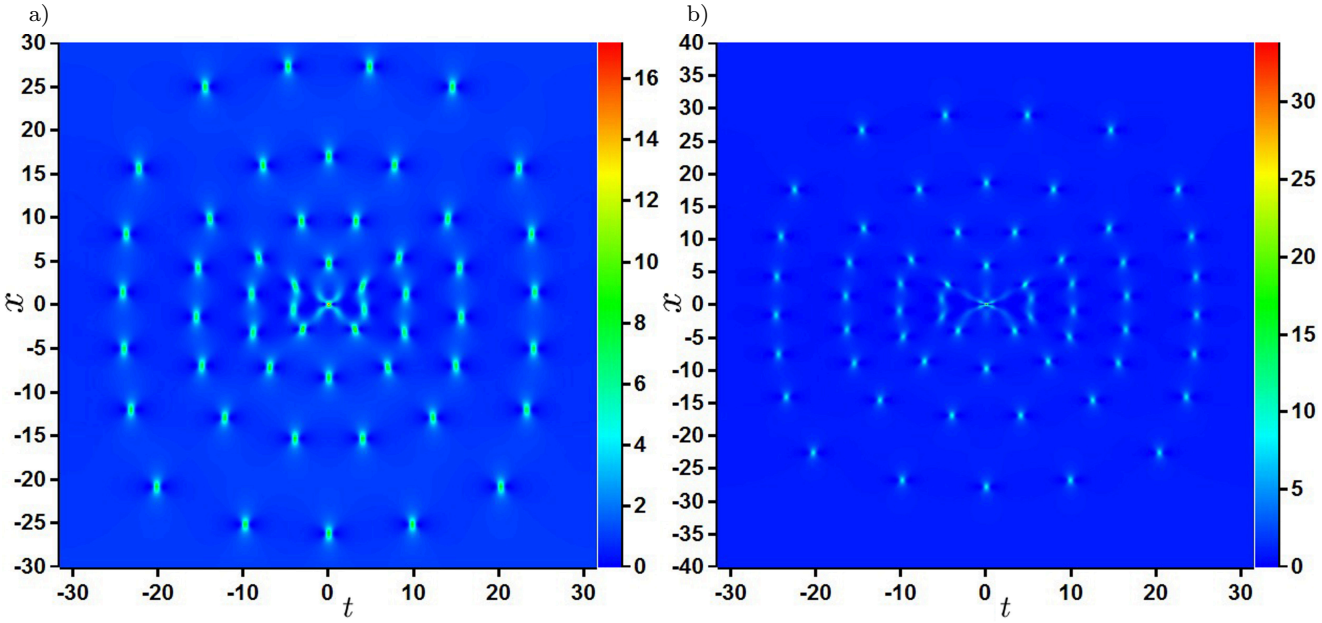


Fig. 3: Rogue wave clusters on the uniform background having four ellipses ($m = 4$) around $n - 2m$ order rogue wave, formed at the origin $(0, 0)$ of the $(x, t)$ plane. Shifts are obtained for $X_{j4} = 10^6$. The orders of Darboux transformation and the Akhmediev breather representing the high intensity central peak are: (a) $n = 10$ with the second-order rogue wave, and (b) $n = 11$ with the third-order rogue wave.

ring, which first increases but then saturates and finally starts to decline slowly. Therefore, we differ the two regions in the $(x, t)$ plane: the first one (I) is roughly estimated as the half-plane before the interception of $R_{x1}$ and $R_{x2}$ curves. In this region the cluster has a regular "concentric ellipses" - like shape. For $\omega = 0.1$, the region I is determined by $x_{\text{shift}} < 11.7$. When $\omega = 0.05$, the region I is given by $x_{\text{shift}} < 23$. The example of a RW cluster in the second region (II) is shown in Fig. 5b. It is clearly seen that the two rings are deformed and thus no longer elliptical in shape. In Figs. 5c and 5d the $R_{x1}$ and $R_{x2}$ dependence is shown for the case of RW2 ad RW3 at the center, respectively, only in the region I where the radial symmetry is preserved.

In Fig. 6a we plot the graph of $R_x$ as a function of $x_{\text{shift}}$ in the case of three rings around a RW2 cluster ($n = 8$ and $m = 3$). We see that the vertical semi-axis of the first and third ellipses is an increasing function of the evolution shift, in contrast to $R_{x2}$. In Fig. 6b the RW2 with four rings is analyzed ($n = 10$ and $m = 4$). Graphs in both figures are computed in region I. Our conclusion is that $x$ position of AB1 (with $t =$

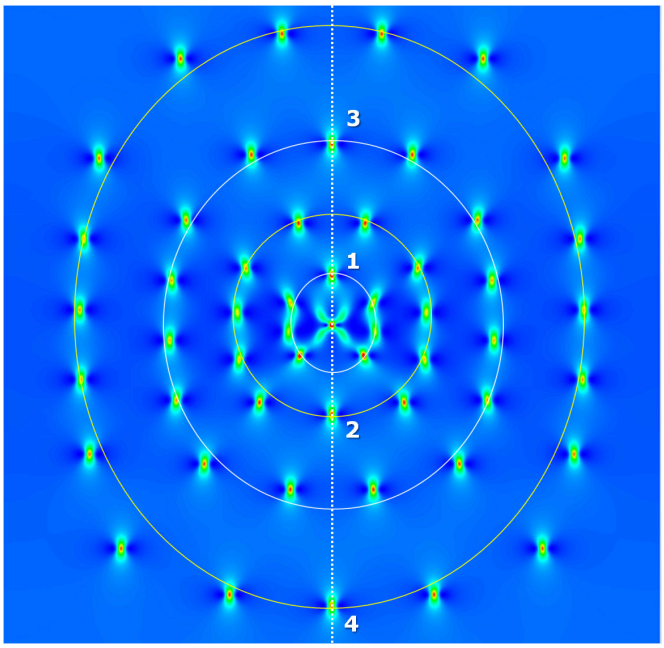


Fig. 4: Quadruple-elliptic rogue wave cluster, obtained for $n = 10$ and $m = 4$, with numbers 1, 2, 3, and 4 indicating the single order Akhmediev breathers located at $t = 0$ on each ellipse. The distance along $x$-axis between the RW center at $(0, 0)$ and the maximum of the breather labeled with $i$ corresponds to the vertical semi-axis $R_{xi}$ of the $i$-th ellipse.

0) on odd labeled ellipses (1, 3) grows constantly with increasing shift, while $R_x$ of even indexed rings (2, 4) first increases, then saturates and finally slowly declines until the symmetry is broken.

## 5 Multi-elliptic rogue wave clusters on Jacobi elliptic dnoidal background

In this section we show that multi-elliptic RW clusters can be obtained on a periodic background defined by Jacobi elliptic dnoidal function dn by using the modified DT scheme for the NLSE [29]. The seed function used here is $\psi_{\rm dn}(x,t) = {\rm dn}(t,g)e^{i(1-g^2/2)x}$, where $g$ is the elliptic modulus and $m_{\rm dn} = g^2$ is the elliptic modulus squared. The choice of eigenvalues and shifts is the same as described in previous sections, but the procedure for calculating $\psi(x,t)$ of order $n$ is different. As explained in [29], the exact analytical values of wave function can be obtained only when $t = 0$. In order to compute $\psi(x, t \neq 0)$ over the entire $(x,t)$ grid, the numerical integration is required. In this work, we use the fourth-order Runge-Kutta algorithm. We manage to obtain a two ring cluster around RW2 ($n = 6$ and $m = 2$) on an elliptic background ($m_{\rm dn} = 0.4^2$) using this numerical procedure. The result is shown in Fig. 7a. We also present the 2-elliptic cluster around RW3 ($n = 7$, $m = 2$, $m_{\rm dn} = 0.4^2$) in Fig. 7b. By a careful look at both 3D plots, one can observe the low amplitude background waves on which the AB1 structures and high-intensity AB2/AB3 peaks are generated.

## 6 Multi-elliptic rogue wave clusters for extended NLSE family

Here we generalize our results to extended family of nonlinear Schrödinger equations [14,15]. It is important to note that the DT technique retains the same recursive relations for the Lax pair and higher-order $\psi$ function as before. We therefore can generate solitons and breathers of any order using the sets of eigenvalues and transverse/evolution shifts as explained above. The intensity distribution of such solutions will differ from the simple cubic NLSE, due to free parameters in the extended families and a bunch of additional dispersion and nonlinear terms, but the procedure for their analytical buildup remains the same. In other words, one can utilize the same algorithm and take identical sets of shifts to compute multi-elliptic RW clusters for any equation from the extended NLSE hierarchy.

Here we show our results for the Hirota equation

$$i\frac{\partial\psi}{\partial x} + \frac{1}{2}\frac{\partial^2\psi}{\partial t^2} + |\psi|^2\psi - i\alpha\left(\frac{\partial^3\psi}{\partial t^3} + 6|\psi|^2\frac{\partial\psi}{\partial t}\right) = 0, \quad (6.1)$$

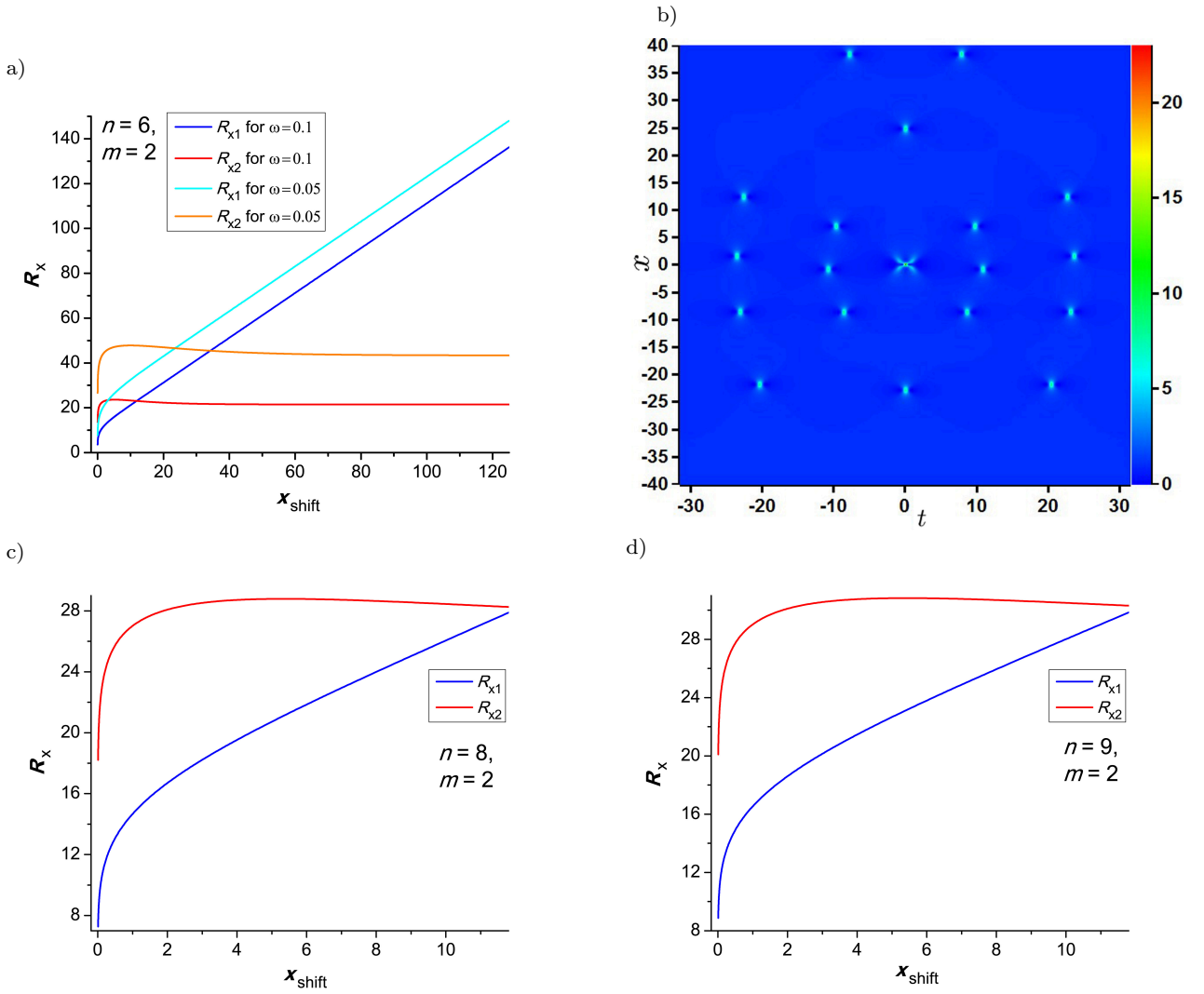


Fig. 5: The dependencies of the vertical semi-axes $R_{x1}$ and $R_{x2}$ on the absolute shift $x_{\text{shift}}$ of the first two components in the Darboux transformation scheme for two ellipses in the RW cluster ($m = 2$). (a) The graphs of $R_{x1}$ and $R_{x2}$ as functions of $x_{\text{shift}}$ for $n = 6$ and two main frequencies: $\omega = 0.1$ and $\omega = 0.05$. The region in which two ellipses in a cluster are deformed roughly begins at $x_{\text{shift}}$ coordinate where $R_{x2}$ saturates and decrease to $R_{x1}$ value (here, $x_{\text{shift}} \approx 11.7$ for $\omega = 0.1$, and $x_{\text{shift}} \approx 23$ for $\omega = 0.05$). (b) The deformed double elliptic cluster obtained for $n = 6$ and $x_{\text{shift}} = 13.5$. (c) The $R_{x1}$ and $R_{x2}$ as functions of $x_{\text{shift}}$ for $n = 8$ in the region of undeformed elliptic cluster. (d) The $R_{x1}$ and $R_{x2}$ as functions of $x_{\text{shift}}$ for $n = 9$ in the region of undeformed elliptic cluster.

where $\alpha$ is the arbitrary real parameter. The only difference in the DT scheme between the cubic NLSE and Hirota's equation is analytical expressions for the Lax pair functions $r$ and $s$, but all recursive relations remain the same, as stated above. The Hirota DT scheme is presented in detail in [19]. Here we generate the multi-elliptic RW cluster on a uniform background with $\psi_0 = e^{ix}$ as the seed. Our main goal is to investigate the cluster appearance when Hirota operator (the term in Eq. 6.1 multiplied by $\alpha$) sets in. For this purpose, we take $\alpha = \pm 0.07$ and build two clusters having RW2 at the $(x, t)$ center, surrounded by two rings ($n = 6$ and $m = 2$). When $\alpha$ is negative, the entire cluster is tilted towards the positive direction of $t$-axis. In addition, the radial symmetry of the central RW2 is broken, since the local maxima in the vicinity of RW2 are more pronounced in the tilted direction.

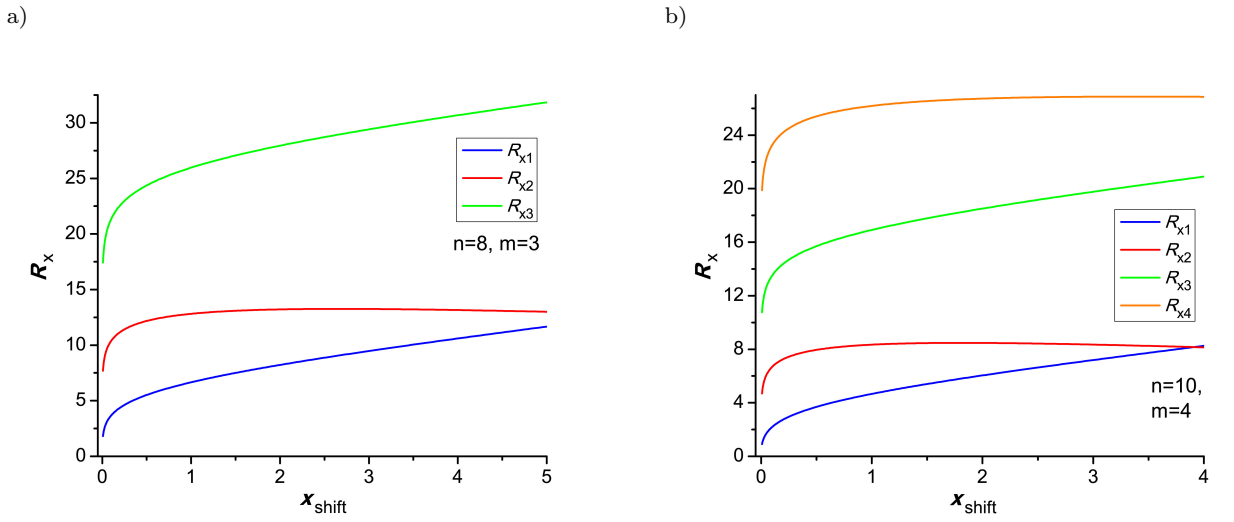


Fig. 6: The dependencies of the vertical semi-axes $R_{xi}$ on the absolute shift $x_{\text{shift}}$ of the first $m$ components in the Darboux transformation scheme of order $n$ for (a) three ellipses in the RW cluster ($n = 8$ and $m = 3$), and (b) four ellipses in the RW cluster ($n = 10$ and $m = 4$).

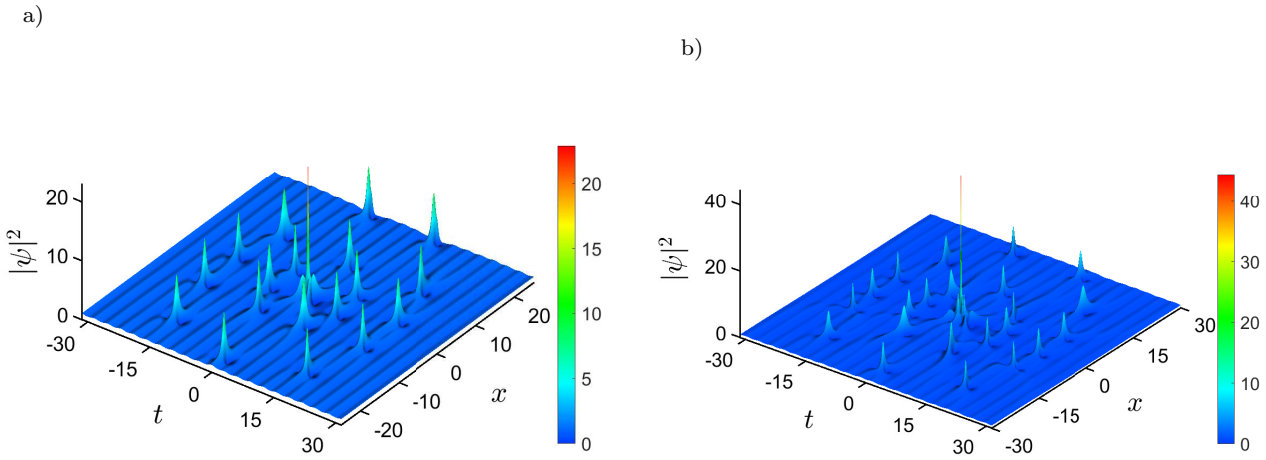


Fig. 7: Rogue wave clusters on the Jacobi elliptic dnoidal background having two ellipses ($m = 2$) around $n - 2m$ order rogue wave formed at the origin $(0, 0)$ of the $(x, t)$ plane. The shifts are computed for $X_{j4} = 10^6$. The elliptic modulus squared is $m_{\text{dn}} = 0.4^2$. The orders of Darboux transformation and Akhmediev breather representing the high intensity central peak are: (a) $n = 6$ with the second-order rogue wave, and (b) $n = 7$ with the third-order rogue wave.

The intensity distribution for $\alpha = -0.07$ is shown in Fig. 8a. If one changes the sign of $\alpha$ then the skew angle will just change the sign. Thus, the vertical axis of both ellipses is tilted by the same amount to the negative $t$ direction. The results for $\alpha = 0.07$ are shown in Fig. 8b. The measured skew angle for $\alpha = \pm 0.07$ is $\theta \approx \pm 18.6°$. In addition, both ellipses are stretched for nonzero $\alpha$, since the distances between AB1s on inner and outer rings (marked in Fig. 4 with 1 and 2) and the central RW2 are bigger than in the NLSE case. For the cubic NLSE ($\alpha = 0$: Fig. 1a) the semi-axis lengths are $R_{x1} = 10.1$ and $R_{x2} = 22$. In the Hirota case, shown in Fig. 8, the semi-axes lengths are $R_1 = 10.76$ and $R_2 = 23.7$. Here we claim that the larger the $\alpha$, the bigger the skew angle and the amount of cluster stretching (results not shown).

The analysis can further be applied on even higher-order equations of the extended NLSE hierarchy using

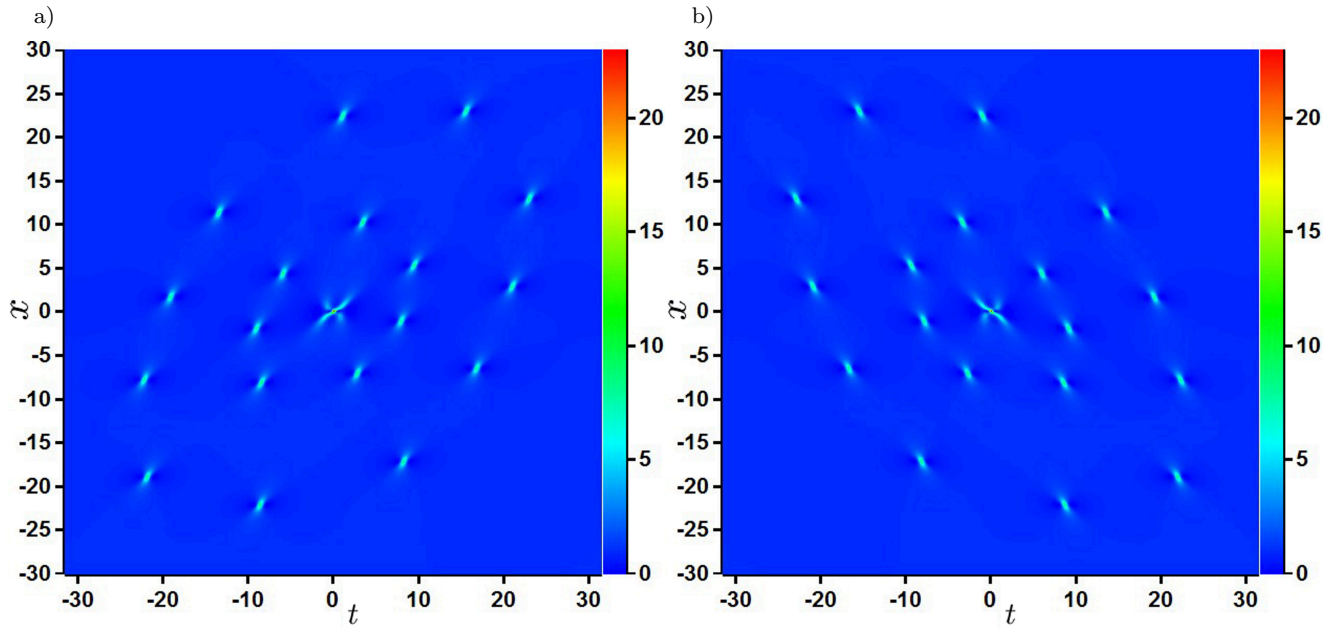


Fig. 8: Double-elliptic rogue wave clusters ($m = 2$) around the second-order RW peak ($n = 6$) at $(0, 0)$ on the uniform background for Hirota equation. The shifts are calculated for $X_{j4} = 10^6$. The free parameter is: (a) $\alpha = -0.07$ and (b) $\alpha = 0.07$.

the same procedure—with similar results. The subject of ongoing research is the influence of higher-order dispersions, additional nonlinearities and real parameters on the overall shape of multi-elliptic RW clusters for this highly nonlinear systems.

## 7 Conclusion

In this paper, we have presented the multi-elliptic rogue wave clusters of nonlinear Schrödinger equation on uniform and nonuniform (Jacobi elliptic dnoidal) backgrounds. We showed that the Darboux transformation scheme of an arbitrary order $n$ (up to $n = 11$) with $m$ equal and nonzero evolution shifts, can produce Akhmediev breathers of $n - 2m$ order positioned at the origin of the $(x, t)$ plane. We showed that this high intensity narrow peak, a central rogue wave, is encircled by $m$ concentric elliptical rings of first-order Akhmediev breathers. The number of AB1s on each ring depends on the ring index and the solution order.

In order to better understand the cluster geometry, we numerically investigated the length of semi-axes of all rings around the central RW. We provided the graphs where distances from RW at $(0, 0)$ to AB1 on the vertical $t = 0$ line at each ellipse were plotted as functions of the absolute evolution shift. Our results suggest that the radial symmetry is destroyed for large evolution shifts.

We next used the modified Darboux transformation scheme to numerically build RW clusters on a periodic background. Although the intensity of higher-order Akhmediev breathers at the center significantly surpass the amplitude of elliptic waves, we were able to observe the weak background oscillations on which the cluster was constructed.

We concluded our analysis by applying the Darboux transformation scheme on Hirota equation. We showed that the Hirota operator introduces the titling and stretching of the entire cluster in a direction determined by the sign of the single real Hirota parameter.

We believe that further research of multi-rogue wave clusters on the cubic NLSEs is warranted in the future, owing to many degrees of freedom offered by the Darboux transformation scheme (the choice of eigenvalues and the spatial and temporal shifts). The research possibilities grow even more if one considers the cluster solutions for the infinite hierarchy of extended nonlinear Schrödinger equations.

## Acknowledgment

This research is supported by the Qatar National Research Fund. S.N.N. acknowledges funding provided by the Institute of Physics Belgrade, through the grant by the Ministry of Education, Science, and Technological Development of the Republic of Serbia. S.Al W. is

supported by the Embassy of Libya in the Republic of Serbia. O.A.A. is supported by the Berkeley Graduate Fellowship and the Anselmo J. Macchi Graduate Fellowship. N.B.A. acknowledges support from project No. 18-11-00247 of the Russian Science Foundation. M.R.B. acknowledges support by the Al-Sraiya Holding Group.

## Conflict of Interest

The authors declare that they have no conflict of interest.

## Data availability

All data generated or analyzed during this study are included in the published article.

## References

1. Fibich, G.: The Nonlinear Schrödinger Equation. Springer, Berlin (2015)
2. Mirzazadeh, M., Eslami, M., Zerrad, E., Mahmood, M.F., Biswas, A., Belić, M.: Optical solitons in nonlinear directional couplers by sine-cosine function method and Bernoulli's equation approach. Nonlinear Dyn. **81**, 1933-1349 (2015)
3. Khalique, C.M: Stationary solutions for nonlinear dispersive Schroödinger equation. Nonlinear Dyn. **63**, 623-626 (2011)
4. Agrawal, G.P.: Applications of nonlinear fiber optics. Academic
5. Kivshar, Y.S., Agrawal, G.P.: Optical Solitons. Academic Press, San Diego (2003)
6. Dudley, J.M., Dias, F., Erkintalo, M., Genty, G.: Instabilities, breathers and rogue waves in optics. Nature Phot. **8**, 755 (2014)
7. Dudley, J.M., Taylor, J.M.: Supercontinuum Generation in Optical Fibers, Cambridge University Press, Cambridge (2010)
8. Kibler, B., Fatome, J., Finot, C., Millot, G., Dias, F., Genty, G., Akhmediev, N., Dudley, J.M.: Observation of Kuznetsov-Ma soliton dynamics in optical fibre. Sci. Rep. 6, 463 (2012)
9. Bao, W.: The nonlinear Schrödinger equation and applications in Bose–Einstein condensation and plasma physics. In: Lecture Note Series, IMS, NUS, vol. **9** (2007)
10. Busch, T., Anglin, J.R.: Dark–bright solitons in inhomogeneous Bose–Einstein condensates. Phys. Rev. Lett. 87, 010401 (2001)
11. Zakharov, V.E.: Stability of periodic waves of finite amplitude on a surface of deep fluid. J. Appl. Mech. Tech. Phys. **9**, (1968)
12. Osborne, A.: Nonlinear ocean waves and the inverse scattering transform. Academic Press (2010)
13. Shukla, P.K., Eliasson, B.: Nonlinear aspects of quantum plasma physics. Phys. Usp. 53, 51 (2010)
14. Ankiewicz A., Kedziora, D.J., Chowdury, A., Bandelow, U., Akhmediev, N.: Infinite hierarchy of nonlinear Schrödinger equations and their solutions. Phys. Rev. E **93**, 012206 (2016)
15. Kedziora, D.J., Ankiewicz, A., Chowdury, A., Akhmediev, N.: Integrable equations of the infinite nonlinear Schrödinger equation hierarchy with time variable coefficients. Chaos **25**, 103114 (2015)
16. Mani Rajan, M.S., Mahalingam, A.: Nonautonomous solitons in modified inhomogeneous Hirota equation: soliton control and soliton interaction. Nonlinear Dyn. 79, 2469– 2484 (2015)
17. Wang, D.-S., Chen, F., Wen, X.-Y.: Darboux transformation of the general Hirota equation: multisoliton solutions, breather solutions and rogue wave solutions. Adv. Differ. Equ. 2016, 67 (2016)
18. Ankiewicz A., Soto-Crespo J.M., Akhmediev N.: Rogue waves and rational solutions of the Hirota equation. Phys. Rev. E **81**, 046602 (2010)
19. Nikolić, S.N., Aleksić, N.B., Ashour, O.A., Belić, M.R., Chin, S.A.: Systematic generation of higher-order solitons and breathers of the Hirota equation on different backgrounds. Nonlinear Dyn. **89**, 1637-1649 (2017)
20. Chowdury, A., Kedziora, D.J., Ankiewicz, A., Akhmediev, N.: Breather solutions of the integrable nonlinear Schrödinger equation and their interactions. Phys. Rev. E **91**, 022919 (2015)
21. Yang, Y., Yan, Z., Malomed, B.A.: Rogue waves, rational solitons, and modulational instability in an integrable fifth-order nonlinear Schrödinger equation. Chaos **25**,
22. Nikolić, S.N., N.B., Aleksić, Ashour, O.A., Belić, M.R., Chin, S.A.: Breathers, solitons and rogue waves of the quintic nonlinear Schrödinger equation on various backgrounds. Nonlinear Dyn. **95**, 2855-2865 (2019)
23. Nikolić, S.N., Ashour, O.A., Aleksić, N.B., Zhang, Y., Belić, M.R., Chin, S.A.: Talbot carpets by rogue waves of extended nonlinear Schrödinger equations. Nonlinear Dyn. **97**, 1215 (2019)
24. Akhmediev, N.N., Korneev, V.I.: Modulation instability and periodic solutions of the nonlinear Schrödinger equation. Theor. Math. Phys. **69**, 1089 (1986)
25. Akhmediev, N., Eleonskii, V., Kulagin, N.: Exact first-order solutions of the nonlinear Schrödinger equation. Theor. Math. Phys. **72**, 809 (1987)
26. Zakharov, V.E., Shabat, A.B.: Exact theory of two-dimensional self-focusing and one-dimensional self-modulation of waves in nonlinear media. J. Exp. Theor. Phys. **34**, 62 (1972)
27. Matveev, V.B., Salle, M.A.: Darboux transformations and solitons. Berlin-Heidelberg: Springer (1991)
28. Kedziora, D.J., Ankiewicz, A., Akhmediev, N.: Circular rogue wave clusters. Phys. Rev. E **84**, 056611 (2011)
29. Kedziora D.J., Ankiewicz A., Akhmediev N.: Rogue waves and solitons on a cnoidal background. Eur. Phys. J. Special Topics **223**, 43-62 (2014)
30. Chin, S.A., Ashour, O.A., Nikolić, S.N., Belić, M.R.: Peak-height formula for higher-order breathers of the nonlinear Schrödinger equation on nonuniform backgrounds. Phys. Rev. E **95**, 012211 (2017)
31. Peregrine, D.H.: Water waves, nonlinear Schrödinger equations and their solutions. J. Austral. Math. Soc. B **25**, 16 (1983)
32. Garrett, C., Gemmrich, J.: Rogue waves. Phys. Today. **62**, 62 (2009)
33. Solli, D.R., Ropers, C., Jalali, B.: Active Control of Rogue Waves for Stimulated Supercontinuum Generation. Phys. Rev. Lett. **101**, 233902 (2008)
34. Dudley, J.M., Genty, G., Eggleton, B.J.: Harnessing and control of optical rogue waves in supercontinuum generation. Opt. Express **16**, 3644 (2008)

35. Ganshin, A.N., Efimov, V.B., Kolmakov, G.V., Mezhov-Deglin, L.P., McClintock, P.V.E.: Observation of an Inverse Energy Cascade in Developed Acoustic Turbulence in Superfluid Helium. Phys. Rev. Lett. **101**, 065303 (2008)
36. Bludov, Y.V., Konotop V.V., Akhmediev, N.: Matter rogue waves. Phys. Rev. A. **80**, 033610 (2009)
37. Akhmediev N., et al.: Roadmap on optical rogue waves and extreme events. J. Opt. **18**, 063001 (2016)
38. Fleischhauer, M., Imamoglu, A., Marangos J.P.: Electromagnetically induced transparency: Optics in coherent media. Rev. Mod. Phys. **77**, 633-673 (2005)
39. Nikolić, S.N., Radonjić, M., Krmpot, A.J., Lučić, N.M., Zlatković, B.V., Jelenković, B.M.: Effects of a laser beam profile on Zeeman electromagnetically induced transparency in the Rb buffer gas cell. J. Phys. B: At. Mol. Opt. Phys. **46**, 075501 (2013)
40. Krmpot, A.J., Ćuk, S.M., Nikolić, S.N., Radonjić, M., Slavov D.G., Jelenković, B.M.: Dark Hanle resonances from selected segments of the Gaussian laser beam cross-section. Opt. Express **17**, 22491-22498 (2009)
41. Li, Z.-Y., Li, F.-F., Li, H.-J.: Exciting rogue waves, breathers, and solitons in coherent atomic media. Commun. Theor. Phys. **72**, 075003 (2020)
42. Kedziora, D.J., Ankiewicz, A., Akhmediev, N.: Rogue wave triplets. Phys. Lett. A **375**, 2782 (2011)
43. Kedziora, D.J., Ankiewicz, A., Akhmediev, N.: Triangular rogue wave cascades. Phys. Rev. E **86**, 056602 (2012)
44. Dubard, P., Gaillard, P., Klein, C., Matveev, V.B.: On multi-rogue wave solutions of the NLS equation and positon solutions of the KdV equation. Eur. Phys. J. Special Topics **185**, 247 (2010)
45. Ohta Y., Yang, J.: General high-order rogue waves and their dynamics in the nonlinear Schrödinger equation. Proc. R. Soc. A **468**, 1716 (2012)
46. Gaillard, P.: Degenerate determinant representation of solutions of the nonlinear Schrödinger equation, higher order Peregrine breathers and multi-rogue waves. J. Math. Phys. **54**, 013504 (2013)
47. Ankiewicz, A., Akhmediev, N.: Multi-rogue waves and triangular numbers. Romanian Reports in Physics **69**, 104 (2017)
48. Kedziora, D.J., Ankiewicz, A., Akhmediev, N.: Classifying the hierarchy of nonlinear-Schödinger-equation rogue-wave solutions. Phys. Rev. E **88**, 013207 (2013)
49. Akhmediev, N.: Waves that Appear From Nowhere: Complex Rogue Wave Structures and Their Elementary Particles. Frontiers in Physics **8**, 612318 (2021)
50. He, J.S., Zhang, H.R., Wang, L.H., Porsezian, K., Fokas, A.S.: Generating mechanism for higher-order rogue waves. Phys. rev. E **87**, 052914 (2013)
51. Chin, S.A., Ashour, O.A., Belić, M.R.: Anatomy of the Akhmediev breather: Cascading instability, first formation time, and Fermi-Pasta-Ulam recurrence. Phys. Rev. E **92**, 063202 (2015)